© 2001 The Chemical Society of Japan Bull. Chem. Soc. Jpn., 74, 1635–1639 (2001) 1635

Growth of Strontium Chlorapatite Crystals from a Sodium Chloride Flux

Shuji Oishi,* Mai Mitsuya,† Takaomi Suzuki, Nobuo Ishizawa,†† Juan Carlos Rendon-Angeles,††† and Kazumichi Yanagisawa†††

Department of Environmental Science and Technology, Faculty of Engineering, Shinshu University,
Wakasato, Nagano 380-8553

†Department of Chemistry and Material Engineering, Faculty of Engineering, Shinshu University,
Wakasato, Nagano 380-8553

††Materials and Structures Laboratory, Tokyo Institute of Technology, Nagatsuta, Midori-ku, Yokohama 226-8503

†††Research Laboratory of Hydrothermal Chemistry, Faculty of Science, Kochi University, Akebono, Kochi 780-8520

(Received March 13, 2001)

Large and well-formed crystals of strontium chlorapatite [$Sr_5Cl(PO_4)_3$] were grown for the first time from a sodium chloride flux. The obtained crystals were colorless and transparent. The crystal growth of $Sr_5Cl(PO_4)_3$ was conducted by heating a mixture of solute and flux at 1100 °C for 10 h, and then cooling to 500 °C at a rate of 5 °C h^{-1}. Hexagonal prismatic crystals with lengths of up to 8.6 mm and widths of 2.1 mm were grown from high-temperature solutions containing 0.05–0.9 mol% solute. The most suitable solute content for the growth of prismatic crystals was 0.2 mol%. The prismatic crystals were bounded by the $\{10\bar{1}0\}$ and $\{10\bar{1}1\}$ faces. The aspect ratios were in the region of 1.1 to 4.2. Hexagonal needle crystals with lengths of up to 2.6 mm and widths of 60 μm were obtained during every growth run. The needle crystals were elongated in the $\langle 0001 \rangle$ directions, with aspect ratios ranging from 33 to 66. The major constituents were almost homogeneously distributed in the prismatic and needle crystals. The solubility of $Sr_5Cl(PO_4)_3$ crystals in NaCl flux increased with increasing temperature, reaching about 0.25 mol% solubility at 1100 °C.

Apatites have been important in at least three different fields; fertilizers, phosphors, and biocompatible materials.[1] The formula of apatite allows a wide variety of substitutions.[1] Strontium chlorapatite has the formula $Sr_5Cl(PO_4)_3$ [pentastrontium chloride tris(phosphate)] and its optical properties have been investigated.[2–6] The crystals of $Sr_5Cl(PO_4)_3$ belong to the hexagonal system with space group $P\ 6_3/m$.[7,8]

A crystalline powder of $Sr_5Cl(PO_4)_3$ has been prepared by a solid state reaction method.[9,10] $Sr_3(PO_4)_2$ has been converted in HCl to a mixture of $Sr_5Cl(PO_4)_3$ and $Sr_2P_2O_7$.[11] Strontium hydroxyapatite, $Sr_5(OH)(PO_4)_3$, has been partially converted to $Sr_5Cl(PO_4)_3$ in the presence of tetrachloromethane.[12] Single crystals of $Sr_5Cl(PO_4)_3$ have been grown by the $SrCl_2$ flux method.[2–4,6,7,13,14] The form of the crystals has been needle-like.[7,13,14] No report on the growth of $Sr_5Cl(PO_4)_3$ crystals from a NaCl flux has been published. The solubility of $Sr_5Cl(PO_4)_3$ crystals in NaCl flux has not yet been reported.

We have, for the first time, grown well-formed crystals of $Ca_5Cl(PO_4)_3$ and $Ba_5Cl(PO_4)_3$ apatites from a NaCl flux.[15,16] The obtained crystals were divided into two distinct morphological types: prisms and needles. The hydrothermal ion exchange of Cl^- by OH^- in the flux-grown $Ca_5Cl(PO_4)_3$ crystals was completed at low temperature of 500 °C, and resulted in the formation of $Ca_5(OH)(PO_4)_3$ crystals.[17] In addition, the $Ca_5Cl(PO_4)_3$ crystals were completely converted to fluorapatite, $Ca_5F(PO_4)_3$, crystals by the ion exchange of Cl^- with F^- under hydrothermal conditions.[18]

In this work, NaCl was chosen as a flux to grow crystals of $Sr_5Cl(PO_4)_3$ on the basis of our experience in growing $Ca_5Cl(PO_4)_3$ and $Ba_5Cl(PO_4)_3$ crystals.[15,16] Sodium chloride has a low melting point with sufficient solubility in water and low toxicity to humans. Sodium chloride was expected to be a good flux.

The present paper describes the growth of $Sr_5Cl(PO_4)_3$ crystals from a NaCl flux. The effect of the solute content on crystal growth was studied. The morphology, density, and imperfections of the resulting crystals were examined. The solubility of $Sr_5Cl(PO_4)_3$ crystals in NaCl flux was also measured.

Experimental

Flux Growth. Reagent-grade $(NH_4)_2HPO_4$, $SrCO_3$, $SrCl_2$, and NaCl were used for the flux growth of $Sr_5Cl(PO_4)_3$ crystals. A mixture of $6(NH_4)_2HPO_4 + 9SrCO_3 + SrCl_2$ powders was used as a solute. Sodium chloride powder was used as the flux. Mixtures containing solutes of 0.05 to 0.9 mol% were prepared in 0.05 or 0.1 mol% increments. The masses of the mixtures were approximately 25.0–26.1 g (25.0 g as $Sr_5Cl(PO_4)_3$–NaCl). The mixtures were put into 30 cm^3 platinum crucibles. After the lids were fitted, the crucibles were placed in an electric furnace with silicon carbide heating elements. The crucibles were heated to 1100 °C at a rate of about 45 °C h^{-1}, held at this temperature for 10 h, and then cooled to 500 °C at a rate of 5°C h^{-1}. When the cooling program was completed, the crucibles were allowed to cool down to room temperature. The crystalline products were then separated by dissolving the flux in warm water.

Characteristics. The obtained crystals were examined using an optical microscope and a scanning electron microscope (SEM). The crystal phases were identified by X-ray diffraction (XRD). The length, L (parallel to the $\langle 0001 \rangle$ directions), and width, W (perpendicular to the $\langle 0001 \rangle$ directions), of the $Sr_5Cl(PO_4)_3$ crystals grown were measured. Based on the aspect ratio (L / W) of the crystals, they were divided into two morphological types: prisms with $L / W \leqq 10$ and needles which had $L / W > 10$. After each growth run, the average length (L_{av}) and width (W_{av}) of the first 30 largest crystals with prismatic or needle forms were calculated. The XRD data of the orientated crystals were obtained. The interfacial angles of the crystals were also measured by use of optical micrographs of grown crystals. The density of each crystal was determined pycnometrically. A SEM equipped with an energy dispersive X-ray spectrometer (EDS) was used to study any variations in the concentration of the major constituents in the grown crystals.

Solubility. The solubility of $Sr_5Cl(PO_4)_3$ crystals in NaCl flux was determined by measuring the mass loss of $Sr_5Cl(PO_4)_3$ in NaCl melts at different temperatures between 700 and 1100 °C. Mixtures of excess crystals (1–4 mm in length, about 1 g) of $Sr_5Cl(PO_4)_3$ and NaCl powder (about 5 g) were put into platinum vessels. After the mixture was heated for 3 h at a preset temperature, undissolved crystals were present upon quenching. The undissolved crystals were separated from the solidified saturated solution in warm water and reweighed. The loss in mass due to dissolution represents the solubility at that temperature. The eutectic temperature of the $Sr_5Cl(PO_4)_3$–NaCl system was determined on the basis of differential thermal analysis (DTA) curves.

Results and Discussion

Flux Growth of $Sr_5Cl(PO_4)_3$ Crystals. Large and well-formed prism- and needle-shaped $Sr_5Cl(PO_4)_3$ crystals having lengths of up to 8.6 mm and widths of 2.1 mm were grown from the NaCl flux. The obtained crystals were colorless and transparent. The crystals tended to grow at the bottom of the crucible due to the difference between the densities of the solute and flux. Prismatic crystals were grown from mixtures containing 0.1–0.9 mol% solute. When mixtures containing 0.1–0.25 and 0.3–0.9 mol% solute were used, long prismatic and short prismatic crystals were grown, respectively. Typical long and short prismatic crystals of $Sr_5Cl(PO_4)_3$ are shown in Figs. 1 and 2, respectively. At all growth runs, needle crystals having lengths of up to 2.6 mm were grown. The mixture containing 0.05 mol% solute produced only needle crystals. The relative frequency of occurrence of needle crystals gradually decreased with solute content. Small numbers of needle crystals were grown from the mixture containing 0.9 mol% solute. Needle crystals of $Sr_5Cl(PO_4)_3$ are shown in Fig. 3.

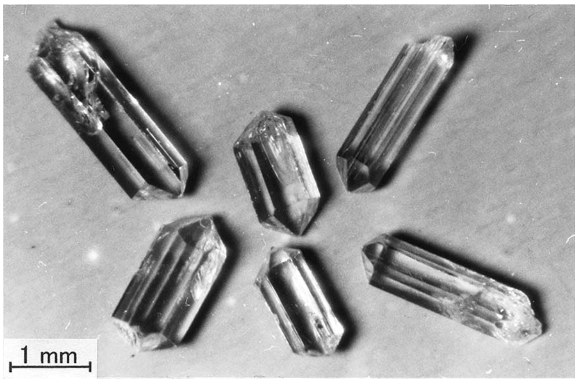

Fig. 1. Optical micrograph showing long prismatic crystals of $Sr_5Cl(PO_4)_3$ grown from NaCl flux.

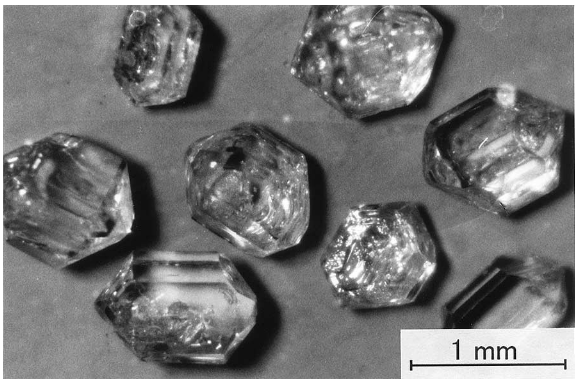

Fig. 2. Optical micrograph showing short prismatic crystals of $Sr_5Cl(PO_4)_3$ grown from NaCl flux.

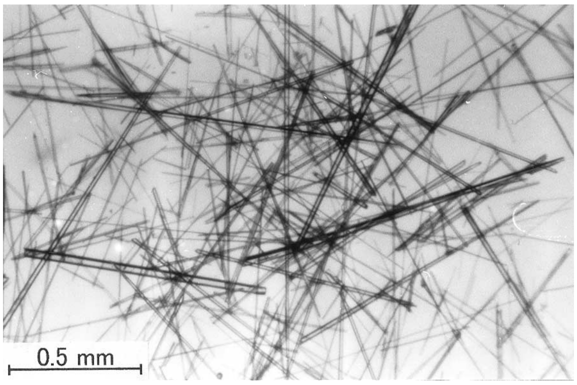

Fig. 3. Optical micrograph showing needle crystals of $Sr_5Cl(PO_4)_3$ grown from NaCl flux.

The average length (L_{av}) and width (W_{av}) of the prismatic crystals are plotted against the solute content in Fig. 4. Large crystals with $L_{av} = 3.8$ mm were grown from a mixture containing 0.2 mol% solute. Any further increase in the solute content resulted in a decrease in the L_{av} value. A mixture containing 0.1 mol% solute resulted in crystals with $W_{av} = 0.7$ mm. The W_{av} value gradually increased with increasing solute content. Mixtures containing a solute of 0.4–0.9 mol% produced crystals with W_{av} values of 1.3–1.6 mm. There was no marked difference among the W_{av} values. The aspect ratios (L_{av}/W_{av}) of the crystals were in the region of 1.1–4.2. The values decreased with increasing solute content. The forms of the crystals varied from long to short prismatic. The size (L_{av} = 3.8 mm) of $Sr_5Cl(PO_4)_3$ crystal is intermediate between those of $Ca_5Cl(PO_4)_3$ (2.4 mm)[15] and $Ba_5Cl(PO_4)_3$ (6.6 mm)[16] crystals. This order is the same as the order obtained for the solubilities in NaCl flux.

Needle crystals of $Sr_5Cl(PO_4)_3$ with dimensions of up to L = 2.6 mm and W = 60 μm were grown from mixtures contain-

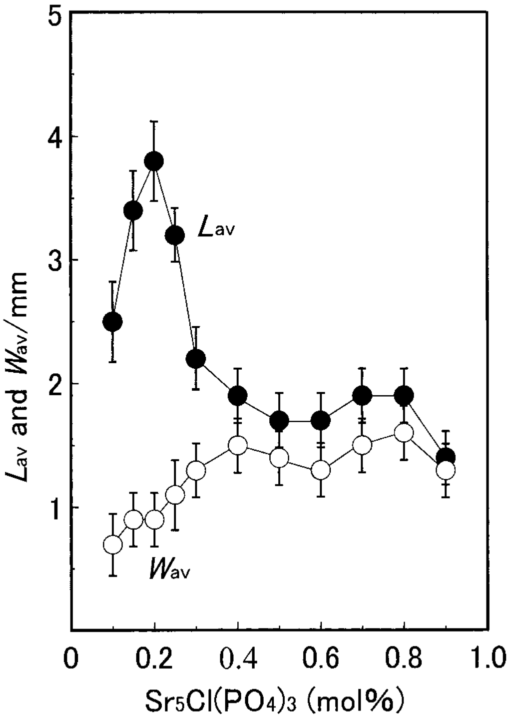

Fig. 4. Variation in average length, L_{av}, and width, W_{av}, of prismatic crystals of $Sr_5Cl(PO_4)_3$ with solute content.

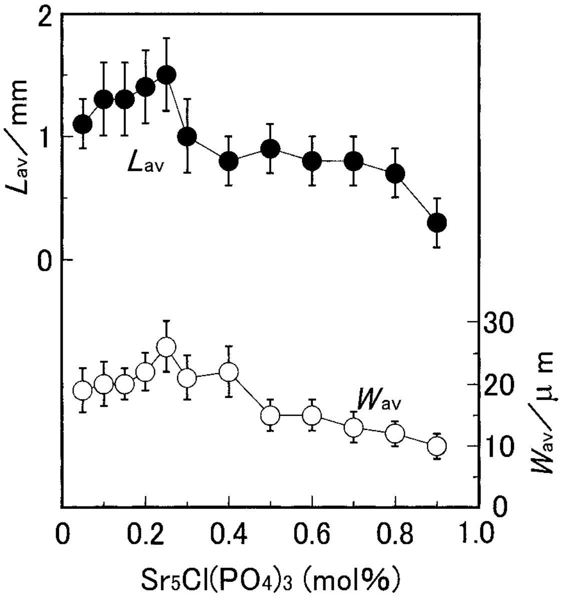

Fig. 5. Variation in average length, L_{av}, and width, W_{av}, of needle crystals of $Sr_5Cl(PO_4)_3$ with solute content.

ing solute of 0.05–0.9 mol%. The average length (L_{av}) and width (W_{av}) of the needle crystals are plotted against solute content in Fig. 5. A mixture containing a solute of 0.05–0.9 mol% produced needle crystals with L_{av} values of 0.3–1.5 mm and W_{av} values of 10–26 μm. The needle crystals grown from solution containing 0.25 mol% solute were relatively large. The aspect ratios of the crystals ranged from 33 to 66. These values were independent of the solute content.

A mixture containing 0.2 mol% solute produced 0.45 g crystals. About 71 mass% of the solute (0.63 g) employed was recovered in the form of prismatic and needle crystals. In a calculation using the starting composition and eutectic composition, the masses of $Sr_5Cl(PO_4)_3$ crystals grown and a powder contained in a eutectic mixture were 0.48 and 0.16 g, respectively. The mass of the obtained crystals was about 94% of the calculated value. The agreement between the observed and calculated mass of grown crystals was good.

During these growth runs, evaporation of the NaCl flux was less than 35 mass%. The evaporation had more or less influence on the growth of $Sr_5Cl(PO_4)_3$ crystals. In practice, a combination of slow cooling with evaporation of the flux produced crystals of $Sr_5Cl(PO_4)_3$. The platinum crucibles were found to be undamaged after use. The NaCl flux did not attack the crucibles. The resulting crystals could be readily separated from the flux in warm water because NaCl was easily soluble.

Characteristics of the $Sr_5Cl(PO_4)_3$ Crystals. The obtained prismatic and needle crystals were identified as $Sr_5Cl(PO_4)_3$ by their XRD patterns, as shown in Fig. 6a and 6d, using data given on the JCPDS card.[8]

The prismatic crystals of $Sr_5Cl(PO_4)_3$ had a form of a hexagonal prism with pyramidal end faces. The surfaces of these crystals were very flat. A typical example is shown in Fig. 7. In order to determine the Miller indices of the crystal faces, orientated crystals were investigated by the XRD method. Figure 6b shows the XRD pattern of the orientated prismatic crystals. The diffraction intensities of the $(20\bar{2}0)$, $(30\bar{3}0)$, and $(40\bar{4}0)$ planes were predominant, indicating that the indices of the prismatic faces were $\{10\bar{1}0\}$. The interfacial angles between the prismatic and pyramidal faces were 50 ± 1°. This value was in good agreement with the calculated interfacial angle of 50.2° between the $\{10\bar{1}0\}$ and $\{10\bar{1}1\}$ faces. On the basis of the XRD data and interfacial angle measurements, it was concluded that the prismatic crystals were bounded by the $\{10\bar{1}0\}$ and $\{10\bar{1}1\}$ faces. The prismatic crystals were elongated in the $\langle 0001 \rangle$ directions. This morphology is similar to those of the $Ca_5Cl(PO_4)_3$ crystals grown from NaCl and $CaCl_2$ fluxes[15,19] and $Ca_5F(PO_4)_3$ crystals grown from a KF flux by a slow-cooling method.[20] Furthermore, the needle crystals of $Sr_5Cl(PO_4)_3$ were also bounded by well-developed six-sided faces. Typical examples are shown in Fig. 8. The XRD patterns of orientated needle crystals again had predominant diffraction intensities at the $(20\bar{2}0)$, $(30\bar{3}0)$, and $(40\bar{4}0)$ planes, as shown in Fig. 6c, though weak diffraction intensities at the $(10\bar{1}0)$, $(10\bar{1}2)$, $(30\bar{3}3)$, and $(20\bar{2}4)$ planes were also observed. It was found that the indices of the side faces were $\{10\bar{1}0\}$. The indices of the six-sided faces of the needle crystals were the same as those of the prismatic crystals. The needle crystals were elongated in the $\langle 0001 \rangle$ directions. On the other hand, the end faces of the needle crystals were not always flat.

Variations in the concentration of the major constituents in the grown $Sr_5Cl(PO_4)_3$ crystals were investigated by the EDS method. Figures 9a and 9b show a SEM photograph and EDS line profiles of the $Sr_5Cl(PO_4)_3$ crystal, respectively. Strontium, phosphorus, and chlorine atoms were distributed almost homogeneously. According to the results, it was considered that oxygen atoms were also distributed almost homogeneously. Flux inclusions were rarely found in the crystals.

Based on the powder XRD data, the lattice parameters of the

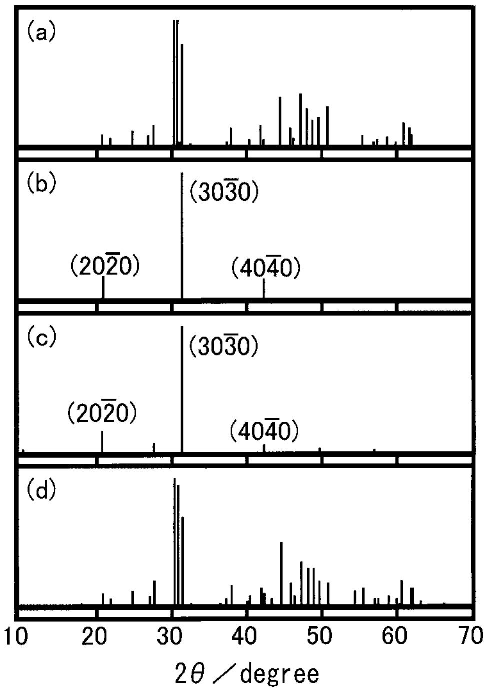

Fig. 6. XRD patterns (Cu *K*α) of $Sr_5Cl(PO_4)_3$ crystals. (a): Pulverized crystallites of prismatic and needle crystals, (b): Orientated prismatic crystals, (c): Orientated needle crystals, and (d): JCPDS data.[8]

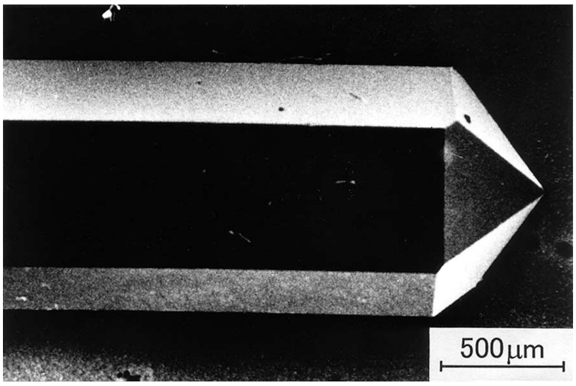

Fig. 7. SEM photograph showing a hexagonal prism with pyramidal end faces of $Sr_5Cl\ (PO_4)_3$.

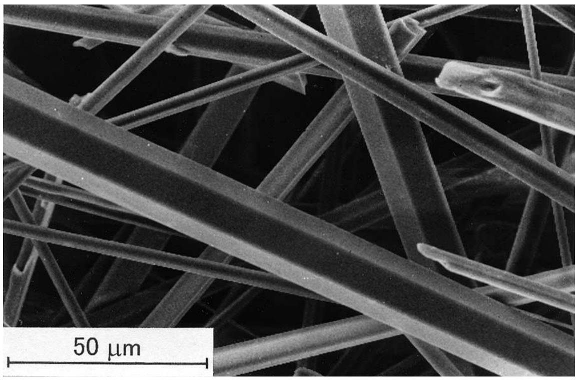

Fig. 8. SEM photograph showing six-sided needles of $Sr_5Cl(PO_4)_3$ crystals.

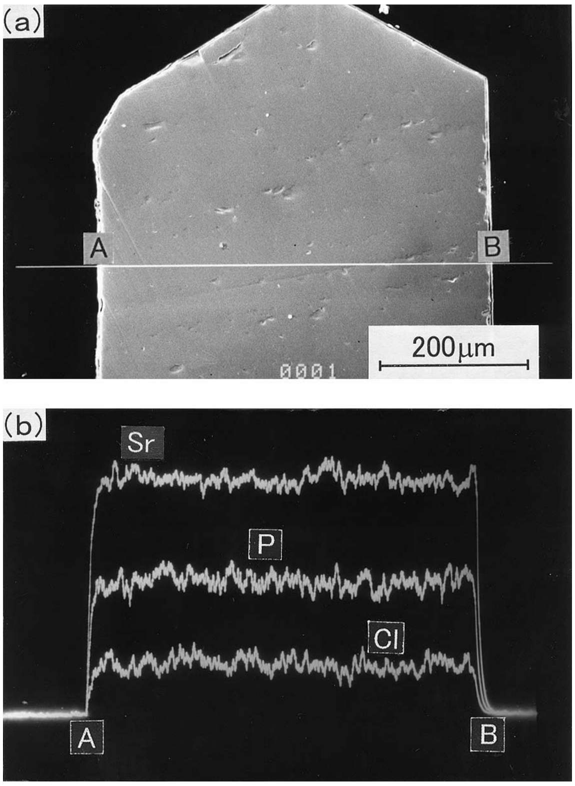

Fig. 9. SEM photograph (a) showing cross sectional interface of $Sr_5Cl(PO_4)_3$ crystal and EDS line profiles (b) of Sr, P, and Cl analyzed along the line between A and B.

$Sr_5Cl(PO_4)_3$ crystals were $a = 9.954 \pm 0.002$ Å and $c = 7.167 \pm 0.002$ Å. These values agree approximately with those ($a = 9.859$ Å and $c = 7.206$ Å,[7] $a = 9.950$ Å and $c = 7.175$ Å[8]) from the literature. The density was pycnometrically determined to be 4.09 ± 0.02 g cm^{-3}. This was in good agreement with the calculated (4.10 g cm^{-3}) and literature (4.095 g cm^{-3})[8] values. The observed lattice parameters and density were independent of the crystal forms.

Solubility of $Sr_5Cl(PO_4)_3$ Crystals in NaCl Flux. The temperature dependence of the solubility of $Sr_5Cl(PO_4)_3$ crystals in NaCl flux is shown in Fig. 10. A mixture of $Sr_5Cl(PO_4)_3$ and NaCl did not melt at 700 °C. At 800 °C, $Sr_5Cl(PO_4)_3$ was dissolved in NaCl at a concentration of about 0.05 mol% (about 0.67 g in 100 g NaCl). The solubility gradually increased with temperature, with $Sr_5Cl(PO_4)_3$ reaching a solubility of about 0.25 mol% (about 3.31 g in 100 g NaCl) at 1100 °C. The obtained solubility curve had an appreciable temperature coefficient of solubility. Therefore, $Sr_5Cl(PO_4)_3$ could be crystallized by slow-cooling of the solutions. Thus, it was confirmed in solubility experiments that NaCl was a suitable flux for growing $Sr_5Cl(PO_4)_3$ crystals.

An endothermic peak appeared at 795 ± 5 °C on the DTA curve obtained during heating a mixture of $Sr_5Cl(PO_4)_3$ and NaCl powders. The peak was due to a eutectic reaction. It was found that the eutectic temperature of the $Sr_5Cl(PO_4)_3$–NaCl system was 795 ± 5 °C. Judging from the solubility curve and eutectic temperature, the eutectic composition was considered to be around $Sr_5Cl(PO_4)_3$ (0.05 mol%)– NaCl (99.95 mol%).

Figure 10 shows that mixtures containing 0.05–0.25 mol%

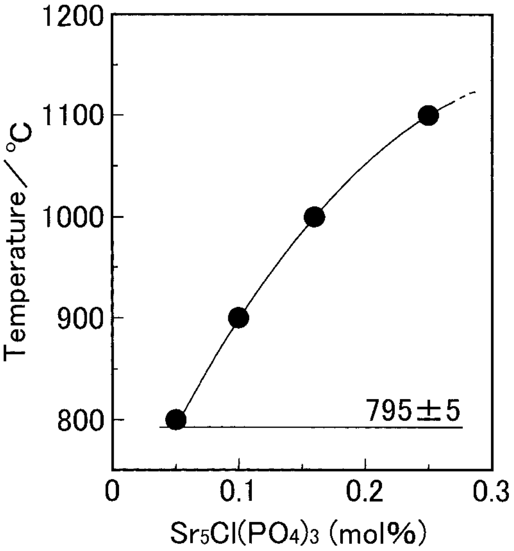

Fig. 10. Solubility of $Sr_5Cl(PO_4)_3$ crystals in NaCl flux as a function of temperature.

solute were unsaturated at a soak temperature of 1100 °C of the flux growth runs. Large and long prismatic crystals were grown from the solutions on subsequent slow cooling. The solubility at 1100 °C corresponds to a starting composition of $Sr_5Cl(PO_4)_3$ (0.25 mol%)–NaCl (99.75 mol%). In the case of mixtures containing 0.3 to 0.9 mol% solute, the solution was incomplete at this soak temperature. The sizes of the grown crystals appeared to be related to the presence of undissolved solute particles. The solubility (0.25 mol%) of $Sr_5Cl(PO_4)_3$ in NaCl at 1100 °C is intermediate between those of $Ca_5Cl(PO_4)_3$ (0.15 mol%)[15] and $Ba_5Cl(PO_4)_3$ (1.9 mol%).[16]

Preliminary experiments confirmed that maintaining a given temperature for 3 h was sufficient for equilibration. The evaporation of NaCl was less than 9 mass% during these solubility experiments. The evaporation had little influence on the solubility.

Conclusions

Strontium chlorapatite, $Sr_5Cl(PO_4)_3$, crystals were grown from a NaCl flux for the first time. Colorless and transparent $Sr_5Cl(PO_4)_3$ crystals with lengths of up to 8.6 mm and widths of 2.1 mm were obtained from high-temperature solutions containing a solute of 0.05–0.9 mol%. The resulting crystals were of two morphological types: prism and needle. The crystal sizes of prismatic crystals were dependent on the solute content. The solubility of $Sr_5Cl(PO_4)_3$ crystals in NaCl flux increased with increasing temperature. Sodium chloride was found to be a suitable flux to grow these crystals.

This work was supported by a grant from the Salt Science Foundation, No. 0004, and a Grant-in-Aid for Scientific Research (C) No. 10650823 from the Ministry of Education, Science, Sports and Culture. A part of this work was carried out under the Collaborative Research Project of the Materials and Structures Laboratory, Tokyo Institute of Technology.

References

1 D. M. Roy, L. E. Drafall, and R. Roy, "Phase Diagrams : Materials Science and Technology," ed by A. M. Alper, Academic Press, New York (1978), Vol. V, pp. 185–239.

2 R. Borromei, L. Oleari, and P. Day, *J. Chem. Soc., Faraday Trans. 2*, **75**, 401 (1979).

3 R. Borromei and E. Fisicaro, *Gazz. Chim. Ital.*, **109**, 191 (1979).

4 R. Borromei and L. Oleari, *J. Chem. Soc., Faraday Trans. 2*, **77**, 1563 (1981).

5 E. L. Benitez, D. E. Husk, S. E. Schnatterly, and C. Tarrio, *J. Appl. Phys.*, **70**, 3256 (1991).

6 J. A. Capobianco, G. Cormier, R. Moncorge, H. Manaa, and M. Bettinelli, *Appl. Phys. Lett.*, **60**, 163 (1992).

7 K. Sudersanan and R. A. Young, *Acta Crystallogr., Sect. B*, **30**, 1381 (1974).

8 JCPDS card 16-666.

9 B. E. Hunt and A. H. McKeag, *J. Electrochem. Soc.*, **106**, 1032 (1959).

10 I. Khattech and M. Jemal, *Thermochim. Acta*, **298**, 17 (1997).

11 A. H. Hoekstra, W. L. Wanmaker, and J. G. Verriet, *J. Inorg. Nucl. Chem.*, **32**, 2445 (1970).

12 S. Sugiyama, T. Minami, H. Hayashi, M. Tanaka, and J. B. Moffat, *J. Solid State Chem.*, **126**, 242 (1996).

13 L. H. Brixner and J. F. Weiher, *J. Solid State Chem.*, **2**, 55 (1970).

14 L. H. Brixner, *Inorg. Syn.*, **14**, 126 (1973).

15 S. Oishi and I. Sugiura, *Bull. Chem. Soc. Jpn.*, **70**, 2483 (1997).

16 S. Oishi, N. Michiba, N. Ishizawa, J. C. Rendon-Angeles, and K. Yanagisawa, *Bull. Chem. Soc. Jpn.*, **72**, 2097 (1999).

17 K. Yanagisawa, J. C. Rendon-Angeles, N. Ishizawa, and S. Oishi, *Am. Mineral.*, **84**, 1861 (1999).

18 J. C. Rendon-Angeles, K. Yanagisawa, N. Ishizawa, and S. Oishi, *Chem. Mater.*, **12**, 2143 (2000).

19 S. Oishi and T. Kamiya, *Nippon Kagaku Kaishi*, **1993**, 1129.

20 S. Oishi and T. Kamiya, *Nippon Kagaku Kaishi*, **1994**, 800.